

Quantum Effects in Ultrafast Electron Transfers within Cryptochromes

Thiago Firmino,^a Etienne Mangaud,^{a,b} Fabien Cailliez,^a Adrien Devolver,^{a,c} David Mendive-Tapia,^d Fabien Gatti,^d Christoph Meier,^b Michèle Desouter-Lecomte,^{a,e} Aurélien de la Lande^a

a: Laboratoire de Chimie Physique, CNRS, Université Paris-Sud, Université Paris Saclay, Orsay F-91405, France.

b: Laboratoire Collisions Agrégats Réactivité, UMR 5589, IRSAMC, Université Toulouse III Paul Sabatier, F-31062, Toulouse, France.

c: Laboratoire de Chimie Quantique et Photophysique, CP160/09, Université Libre de Bruxelles, B-1050 Brussels, Belgium.

d: CTMM, Institut Charles Gerhardt UMR 5253, CNRS/Université de Montpellier, France.

e: Département de Chimie, Université de Liège, Sart Tilman, B6, B-4000 Liège, Belgium.

Supplementary Material

List of supplementary Figures and Tables:

Figure S1: Fluctuation of electronic coupling matrix element (H_{DA}) from different density functional methods for 69 geometries.

Figure S2: Fluctuation of the energy gap (ΔE) from different density functional methods for 69 geometries.

Figure S3: Correlation between electronic coupling matrix element (H_{DA}) from PBE0 50% HF and PBE.

Figure S4: Reorganization energy computed from the variance of the energy gap as a function of the simulation length.

Table S1: Simulation lengths for ET steps 1 and 2 on the initial and final diabatic electronic states for each steps.

Table S2: Contributions to the outer-sphere reorganization energy calculated with eqn (17). The data are computed from simulations performed on state CT1 (respectively CT2) for ET1 (respectively ET2).

Table S3: Contributions to the outer-sphere reorganization energy calculated from the variance of the energy gap for the first ET step when the MD simulation is performed on the CT2 diabatic state.

Table S4: Contributions to the outer-sphere reorganization energy calculated from the variance of the energy gap for the second ET step when the MD simulation is performed on the CT3 diabatic state.

Table S5: Parameters of the Lorentzian functions.

Calibration of Electronic Coupling obtained by Constrained Density Functional Theory

Electronic coupling obtained from cDFT are known to be largely dependent on the amount of exact Fock exchange included in the Kohn-Sham potential. In particular H_{DA} obtained with generalized-Gradient-Approximation functionals can be severely overestimated. On the other hand, to achieve high efficiency in the propagation of cDFT/MM molecular dynamics simulations we employed the Perdew, Burke, Ernzerhof (PBE) GGA functional. We therefore rescaled *a posteriori* the values of the electronic coupling obtained along MD simulations on the PBE Potential Energy Surface. To this end a selection of 69 independent geometries extracted from the simulations was used for benchmark calculations. Single point cDFT/MM calculations were carried out with the following functionals: PBE, B3LYP, BHHLYP, PBE0, PBE0-50 (*i.e.* PBE0 but with a percentage of Fock exchange of 50%) and M06-2X. The electronic couplings (H_{DA}) and the diabatic energy gaps (ΔE) are given in Figures S1 and S2. As expected H_{DA} obtained with the local PBE functional are always larger than that obtained with a hybrid functional. Moreover, the larger the percentage of Fock exchange introduced in the functional the smaller the electronic coupling. On the other hand the diabatic energy gaps are much less dependent on the DFT functional. This justifies our procedure consisting in propagating MD simulations with the cheaper PBE functional and rescaling the electronic coupling in a subsequent step. The scaling factor was determined against the PBE0-50 functional, imposing a zero shift at the origin (Figure S3). A scaling factor of 0.227566 was used.

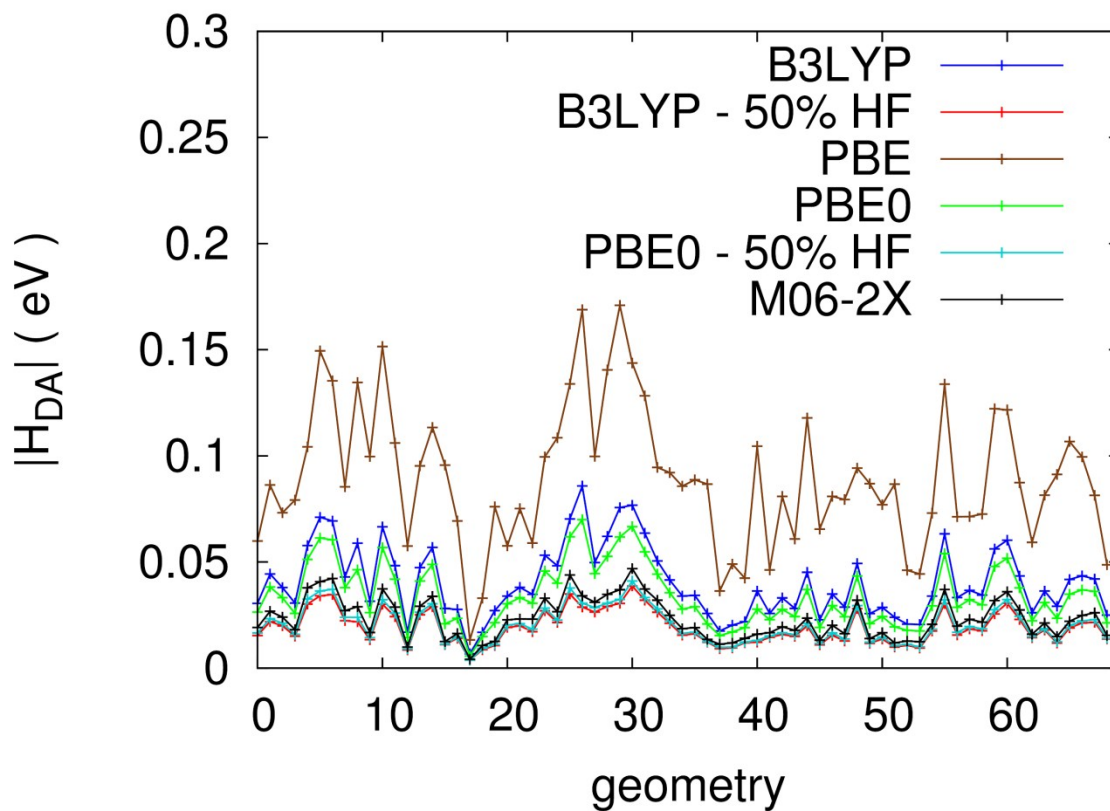


Figure S1: Electronic coupling matrix element (H_{DA}) computed with various GGA and hybrid GGA functionals over a set of 69 geometries extracted from cDFT/MM MD simulations.

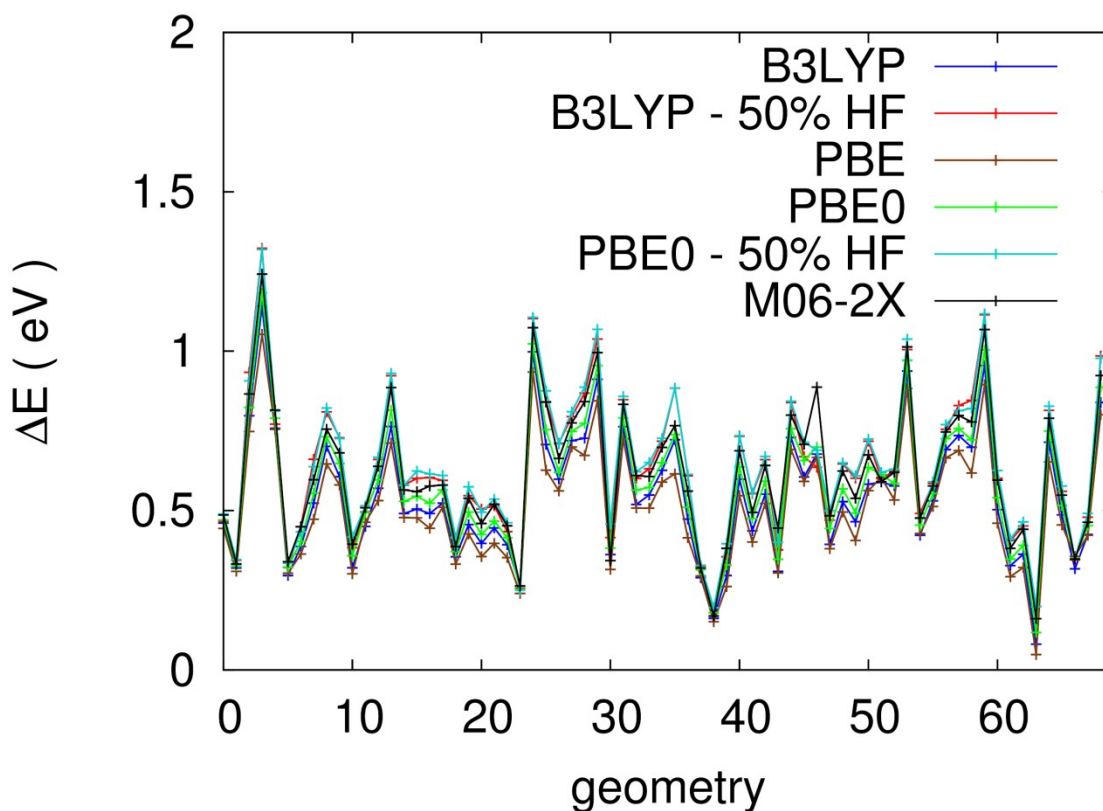


Figure S2: Fluctuation of the energy gap (ΔE) computed with various density functional methods for 69 geometries.

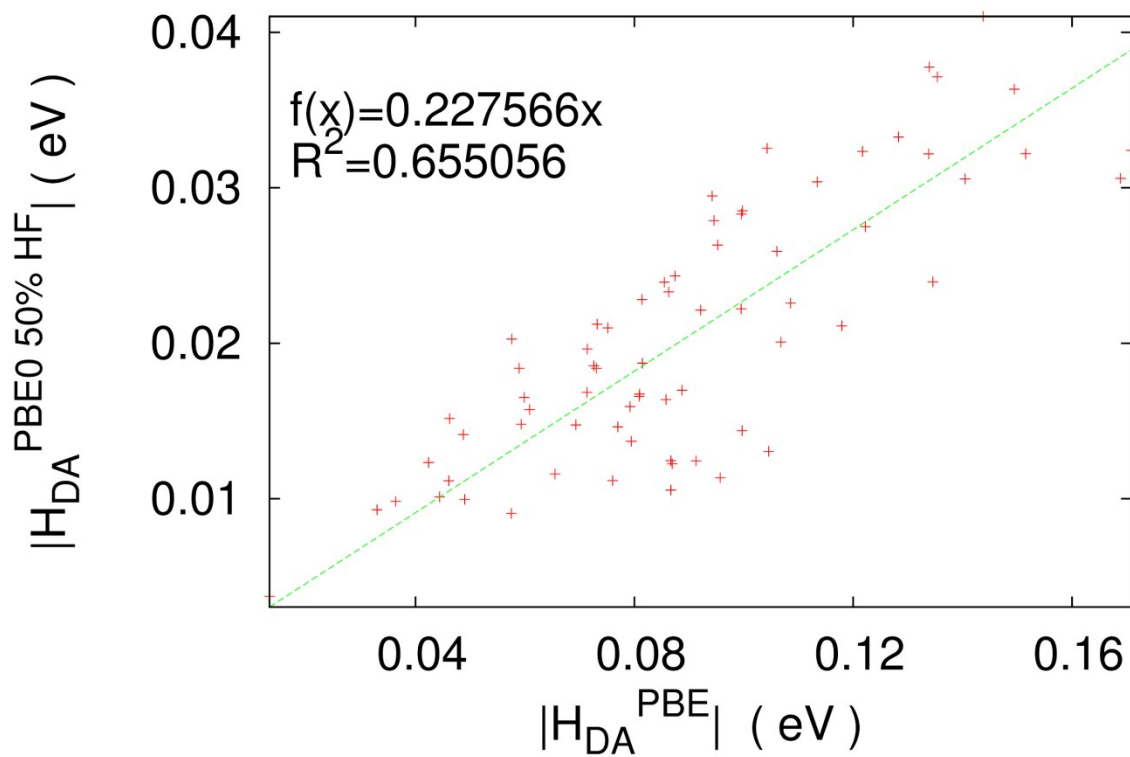


Figure S3: Determination of a scaling factor to correct H_{DA} values obtained with PBE, taking PBE0-50 as a reference.

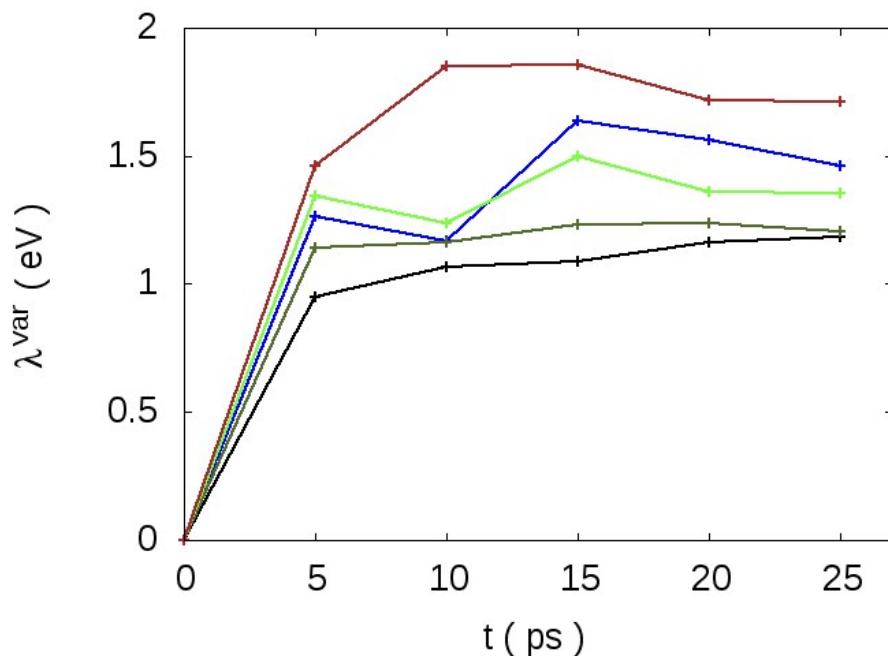


Figure S4: Reorganization energy computed from the variance of the energy gap as a function of the simulation length. We depict the values obtained for the first ET step considering five MD simulations on the first diabatic energy surface.

Table S1 gathers the data obtained from cDFT/MM MD simulations performed on charge transfer state CT2 ($W_{400}; W_{377}^{\circ+}$). The energy gap is defined as the difference between the energies of CT1 and CT2 ($\Delta E^{1-2} = E^{CT2} - E^{CT1}$). See also Table 4 of the main text.

Table S2 gathers the data obtained from cDFT/MM MD simulations performed on CT3 ($W_{377}; W_{324}^{\circ+}$). The energy gap is defined as the difference between the energies of CT3 and CT2 ($\Delta E^{2-3} = E^{CT3} - E^{CT2}$). See also Table 4 of the main text.

Table S3 gathers the parameters of the Lorentzian functions (eq. 30). These Lorentzian functions are used in the quantum dynamical propagation by the hierarchical equations of motion formalism (eq. 32).

state	$W_{377} \rightarrow W_{400}^+$		$W_{324} \rightarrow W_{377}^+$	
	CT1	CT2	CT2	CT3
1	29	28	35	23
2	28	34	26	36
3	29	35	31	37
4	28	31	21	20
5	32	27	29	13
Total	146	155	142	129

Table S1: Simulation lengths for ET steps 1 and 2 (see **Erreur ! Source du renvoi introuvable.** of the main text) on the initial and final diabatic electronic states for each steps. Simulation lengths are given in ps.

ET1	λ'_{FAD}^{var}	λ'_{WAT}^{var}	λ'_{prot}^{var}	λ'_{ATP}^{var}	λ'_{ions}^{var}	λ'_{cross}^{var}
1	0.17	0.88	0.63	0.03	0.03	-0.80
2	0.04	0.94	0.85	0.02	0.03	-0.70
3	0.09	0.65	0.69	0.06	0.04	-0.63
4	0.06	0.57	0.63	0.03	0.06	-0.25
5	0.04	0.76	1.01	0.02	0.02	-0.42
Avg.	0.08	0.76	0.76	0.03	0.04	-0.56
<hr/>						
ET2						
1	0.02	2.45	0.75	0.02	0.03	-1.28
2	0.02	2.15	0.75	0.05	0.05	-1.45

3	0.02	3.81	0.91	0.04	0.04	-1.70
4	0.01	2.13	0.95	0.01	0.11	-2.27
5	0.01	1.32	0.93	0.01	0.02	-1.16
Avg.	0.02	2.37	0.86	0.03	0.05	-1.57

Table S2: Contributions to the outer-sphere reorganization energy calculated with eqn (17). The data are computed from simulations performed on state CT1 (respectively CT2) for ET1 (respectively ET2). All energies are given in eV.

Traj.	λ'_{FAD}^{var}	λ'_{WAT}^{var}	λ'_{prot}^{var}	λ'_{ATP}^{var}	λ'_{ions}^{var}	λ'_{cross}^{var}
1	0.05	0.67	0.69	0.03	0.03	-0.72
2	0.06	1.29	0.88	0.03	0.04	-1.24
3	0.08	0.56	0.57	0.03	0.03	-0.43
4	0.05	0.89	0.75	0.02	0.07	-0.66
5	0.05	0.83	0.67	0.02	0.03	-0.66
Avg.	0.06	0.85	0.71	0.03	0.04	-0.74

Table S3: Contributions to the outer-sphere reorganization energy calculated from the variance of the energy gap for the first ET step when the MD simulation is performed on the CT2 diabatic state. All energies are given in eV.

traj.	λ'_{FAD}^{var}	λ'_{WAT}^{var}	λ'_{prot}^{var}	λ'_{ATP}^{var}	λ'_{iosn}^{var}	λ'_{cross}^{var}
1	0.04	2.06	0.78	0.03	0.03	-1.02
2	0.02	1.42	0.99	0.03	0.02	-0.96

3	0.01	2.35	1.08	0.03	0.04	-1.85
4	0.01	1.07	0.89	0.02	0.18	-1.13
5	0.03	1.44	0.89	0.02	0.04	-1.16
avg.	0.02	1.67	0.93	0.03	0.06	-1.22

Table S4: Contributions to the outer-sphere reorganization energy calculated from the variance of the energy gap for the second ET step when the MD simulation is performed on the CT3 diabatic state. All energies are given in eV.

$p_{1,k}$	$1.377 \cdot 10^{-11}$	$6.117 \cdot 10^{-10}$	$1.233 \cdot 10^{-10}$	$1.490 \cdot 10^{-10}$	$4.414 \cdot 10^{-10}$
$\Omega_{1,k}$	$4.041 \cdot 10^{-4}$	$2.897 \cdot 10^{-3}$	$5.598 \cdot 10^{-3}$	$7.068 \cdot 10^{-3}$	$1.561 \cdot 10^{-2}$
$\Gamma_{1,k}$	$5.776 \cdot 10^{-4}$	$1.368 \cdot 10^{-3}$	$3.441 \cdot 10^{-4}$	$1.277 \cdot 10^{-4}$	$6.207 \cdot 10^{-4}$
$p_{2,k}$	$1.458 \cdot 10^{-11}$	$8.177 \cdot 10^{-10}$	$8.175 \cdot 10^{-10}$	$1.234 \cdot 10^{-10}$	$3.932 \cdot 10^{-10}$
$\Omega_{2,k}$	$3.195 \cdot 10^{-4}$	$3.106 \cdot 10^{-3}$	$6.465 \cdot 10^{-3}$	$7.225 \cdot 10^{-3}$	$1.537 \cdot 10^{-2}$
$\Gamma_{2,k}$	$5.399 \cdot 10^{-4}$	$1.079 \cdot 10^{-3}$	$8.436 \cdot 10^{-4}$	$1.335 \cdot 10^{-4}$	$3.779 \cdot 10^{-4}$

Table S5: Parameters of the Lorentzian functions (eq. 30) $p_{j,k}$, $\Omega_{j,k}$, $\Gamma_{j,k}$